Available online at www.sciencedirect.com

ScienceDirect

Procedia Structural Integrity 13 (2018) 304–310

Structural Integrity Procedia

www.elsevier.com/locate/procedia

ECF22 - Loading and Environmental effects on Structural Integrity

Environmental effects in biaxially orientated Polymethyl Methacrylate

Sze Ki Ng[a]*, Muhammad A. Kamaludin[a], John P. Dear[a], Bamber R. Blackman[a]

[a]*Department of Mechanical Engineering, Imperial Collge London, London,UK SW7 2AZ*

Abstract

Environmental stress cracking (ESC) is commonly found in polymers when submerged in an environment under applied stress. In such conditions, a crack may initiate and propagate from a material defect until it reaches a critical size and causes catastrophic failure. It is known that materials with a denser molecular structure are less prone to ESC, hence amorphous polymers often suffer greatly from this effect. A fracture mechanics approach was employed to investigate the fracture mechanism and crack growth in both air and environment. Two different grades of PMMA (amorphous and biaxially stretched PMMA) were tested in solvents with similar solubility parameters as this is known to hasten crazing. Time for crack initiation and crack speed were obtained and plotted against their corresponding fracture toughness. Thus, the ESC resistance of each material can be compared and component life expectance can also be predicted. To validate the experimental results, scanning electron microscopy (SEM) was used to examine the fracture mechanism of ESC.

© 2018 The Authors. Published by Elsevier B.V.
Peer-review under responsibility of the ECF22 organizers.

Keywords: environmental stress cracking; biaxially orientated PMMA; fracture mechanics; crazing

1. Introduction

Modern aircraft canopies are constructed from transparent polymers such as Polymethyl Methacrylate (PMMA) as lightweight alternative to glass and an economical substitution to Polycarbonate (PC). However, standard amorphous PMMA exhibits a brittle behaviour under loading or impact and is relatively low in strength in comparison to other transparent materials. One recently developed method to improve their mechanical properties is to pre-stretch and

* Sze Ki Ng.
E-mail address: sze.ng11@imperial.ac.uk

2452-3216 © 2018 The Authors. Published by Elsevier B.V.
Peer-review under responsibility of the ECF22 organizers.
10.1016/j.prostr.2018.12.051

force the polymer chains to adopt an ordered arrangement in the direction of the applied stress (Wang et al. 2015). The resultant directional PMMA exhibits desirable properties such as improved toughness, crack resistance, impact resistance, fatigue performance and anti-crazing properties making them attractive for aviation applications. Studies of biaxially orientated PMMA (BOPMMA) sheets are relatively rare.

An aircraft canopy is a critical component needing to withstand the overall stress transmitted to the aircraft body and ensure the safety of the pilots. With a high emphasis on the safety concerns with transparent polymers used for aeronautical applications, this study investigates the damage tolerance design of a biaxially oriented PMMA, YB-DM-10 used for aircraft cockpit applications. In particular, catastrophic failures via environmental stress cracking (ESC) initiated by crazing will be studied. The tensile modulus, tensile strength, glass transition temperature, fracture toughness, fracture energy, crack initiation time and crack speed were measured. The crazing mechanisms have then been identified using scanning electron microscopy.

2. Experimental

2.1. Materials

Two different grades of PMMA namely amorphous and biaxially stretched were investigated. The amorphous PMMA used were 5mm clear Acrylic sheets sourced from RS Component Ltd. The biaxially stretched PMMA, YB-DM-10 were provided by sponsor. The manufacturing process consists of clamping the four edges of a sheet of amorphous PMMA and pre-scratching it simultaneously in both the in-plane directions at an elevated temperature. The resultant mean orientation degree, λ of YB-DM-10 was 70%. This is determined directly from measuring the sheet thickness before, t_1 and after, t_2 the stretching:

$$\lambda = 1 - \sqrt{\left(\frac{t_2}{t_1}\right)} \tag{1}$$

2.2. Mechanical Testing

Uniaxial tensile tests were performed on amorphous PMMAs in accordance with the ISO 527-1 test standard (ISO 527-1:2012 2012) to determine its tensile properties. Specimens were tested at a loading rate of 10 mm/min, force outputs and localised strain measurement from a clip-on extensometer were collected. In the case of BOPMMA, raw data from the uniaxial tensile tests were provided by Beijing Institute of Aeronautical Materials (BIAM). A strain interval of 0.0005-0.0025 was used to calculate the tensile modulus of both materials.

Dual-cantilever dynamic mechanical analysis (DMA) was performed on PMMA to determine its glass transitional temperature. Specimens of dimension 6 x 10 x 60 mm were tested at 1 Hz with an amplitude of 30 μm and temperature range from 0 to 170 ^{o}C. Storage and loss modulus data were obtained across the temperature range to calculate Tan delta, which was used to determine the glass transition temperature.

Three-point bending tests were performed on single edge notched bending (SENB) specimens in accordance with the ISO standard (ISO 13586 2000) to determine the fracture properties. Specimens with a span-to-width, s/w ratio of 4 and nominal crack length-to-width ratio, a/w between 0.45 to 0.55 were tested at a displacement rate of 10 mm/min. A pre-crack was created by broaching from a machined V-notch to ensure a sharp crack-tip prior to testing.

Environmental stress cracking tests were performed in both air and methonal to hasten crazing on PMMA. SENB specimens similar to those used in the three-point bending tests with a/w ≈ 0.35 were tested under load control. A constant pre-defined load hence constant G was applied gradually to the specimen to prevent crack tip blunting from shock loading. Time and voltage data measured from a linear variable differential transformer (LVDT) was used to calculate the crack initiation time, t_i and crack speed, $\dot{a}$.

2.3. Optical Analysis

An optical microscope was used to observe the notch-tip radius, ρ of each pre-crack after broaching. This was to ensure a 'sharp' pre-crack and to avoid any crack-tip with ρ greater than the material crack opening displacement, COD, in the specimens used for testing.

A Hitachi S-3400N scanning electron microscopy (SEM) was used to observe the fracture surface for any crazing mechanisms and used to distinguish between the relaxation-controlled, flow controlled and 'in-air' regions within the crack growth. Each specimen was finely sputter-coated with gold for conductivity. An accelerating voltage of 10kV, working distance of 10 mm, tilt angle of 15° and a magnification of x50 were used on all specimens.

2.4. Data Analysis

A linear elastic fracture mechanics (LEFM) approach was employed to investigate the crack initiation and propagation during ESC. The compliance model from (Kamaludin et al. 2017) was used:

$$C(t) = \frac{\delta(t)}{P} = \frac{16}{E(t)B}\left[\frac{9}{8} + \frac{9}{2}\int_0^x Y^2(x) \cdot x dx\right] = \frac{16}{E(t)B}\varphi(x) \tag{2}$$

where C is the compliance of the sharp-notched specimen at the applied load, P and displacement, δ, E is the Young's modulus, B is the specimen thickness and x is the normalised crack length against specimen width. The bending and shear contribution is expressed by the first term in square brackets, while the second term accounts for the presence of the crack tip and growth. The geometry factor, Y of an SENB specimen under three-point bending condition can be expressed as:

$$Y(x) = 1.93 - 3.07x + 14.53x^2 - 25.11x^3 + 25.8x^4 \tag{3}$$

The compliance of a blunt-notched specimen can be found using the same compliance model. Thus the point of crack initiation can be defined when the compliance ratio between a sharp and blunt notched specimen differs by 2%. Hence, the crack length, a can be found using a straight line fit given $x_b > 0.25$:

$$\frac{C_b}{C} = p(1-x)^2 + q \tag{4}$$

where p and q are the fitting constants used relating to x as shown in table 1.

Table 1. Fitting constants for $x_b > 0.25$ (Kamaludin et al. 2017).

x_b	φ_b	p	q
0.25	1.56	1.86	0.01
0.30	1.76	2.11	0.01
0.35	2.02	2.42	0.02
0.40	2.36	2.83	0.02
0.45	2.81	3.37	0.02
0.50	3.42	4.09	0.03
0.55	4.25	5.09	0.03
0.60	5.44	6.51	0.04

Rearranging the compliance equation, an instantaneous modulus, E can be found. Thus, substituting E into the equation below, the instantaneous fracture toughness throughout the test can be determined:

$$G_C = \frac{K_C^2}{E}(1-v^2) = \frac{\sigma^2 Y^2 a}{E}(1-v^2) \tag{5}$$

where G_C is the fracture energy, K_C is the fracture toughness and v is the Poisson's ratio.

3. Results and Discussion

3.1. Material Properties

Material properties for both amorphous and biaxial PMMA are shown in Table 2.

Table 2. Material properties of PMMA and BOPMMA.

Properties	PMMA	BOPMMA
Tensile Strength, UTS (MPa)	81.5	91.9
Tensile Modulus, E (GPa)	3.85	3.55
Glass Transition Temperature, T_g (°C)	138	140
Fracture Toughness, K_C (MPa√m)	1.01	2.50
Fracture Energy, G_C (J/m^2)	484	1710

The biaxial orientation has greatly improved the material fracture properties from its amorphous form. Also, a 13% increase in tensile strength, UTS was increased from amorphous to BOPMMA due to the increase in chain alignment in the direction of stretch. The decrease in tensile modulus, E from 3.85 to 3.55 MPa after the biaxial stretching process can be explained by the higher ductility in the biaxial material. In other words, at a given stress, the biaxially orientated PMMA can withstand a higher degree of deformation hence experiences a higher strain compared to amorphous PMMA. The glass transition temperature on the other hand are similar in both materials as the biaxial stretching process does not alter the chemical bonds within the material. The fracture properties of PMMA were enhanced with the 70% orientation degree. The fracture toughness, K_C and fracture energy, G_C have increased 150% and 260% respectively from its amorphous to biaxial state.

3.2. Crazing Mechanism

Crazing often nucleates from inherent defects in the material. Resulting voids are interspaced with fibrils. When applied with sufficient energy normal to the plane of crazing, the adjacent fibrils separate forming a crack (Axilrod et al. 1952). This leads to stress concentration at the crack tip and continuous crack growth may occur and lead to brittle fracture. This phenomenon is commonly found in certain polymers if submerged in an environment under applied stress.

The fracture process experienced in environmental stress cracking can be explained by the relaxation-growth model described by (Williams and Marshall 1975; Williams 1984). Three distinct regions labelled as region I, II and III (as shown in fig. 1) can be found on the log G-log crack speed curve. When the ESC specimen is first loaded in region I, the crack propagates slowly, allowing enough time for the environment to flow and submerge the crack tip. Hence, the fracture toughness of the material is independent to the crack speed. In contrast, during the fast crack growth observed in region III, the environment does not reach the crack tip. Thus, crack growth in this region is identical to the 'in-air' behaviour. Region II is the flow controlled transition region whereby the energy required to create two new fracture surfaces is reduced in presence of the environment and becomes limited by its availability. Depending on the model applied, this transition slope has a gradient of either 0.5 or infinity which corresponds to constant speed.

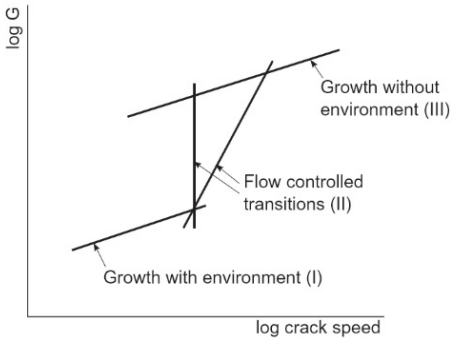

Fig. 1. Three regions of crack growth during ESC (Kamaludin et al. 2017).

3.3. Environmental Stress Cracking

All ESC results are plotted in logarithm scale to allow the identification of the power law relation. Overall, at least five repeats were performed on both materials under each environment except for the case of BOPMMA in air. Only one complete set of data was obtained for BOPMMA in air as the material has a high ESC resistance and often the crack does not propagate through the material under constant load. As cracks propagate in the direction of least resistance; during the biaxial stretching process, polymer chains uncoil from their amorphous state and orient biaxially in the plane of stretch. As reflected by the UTS values, polymer chains oriented longitudinally in the direction of stretch are significantly stronger than those oriented transversely. The fracture mechanism experienced during ESC can be described by the crack opening displacement (COD) criterion at crack initiation and viscoelastic relaxation localised to crack tip during crack propagation. The crack blunting effect may dominate at high crack speed, resulting a crack tip radius exceeding a critical value (Chan and Williams 1983; M.Rink et al. 2003; Alexander and Atteck 2009). As a result, the crack growth will pause under constant load conditions unless more energy is applied to propagate the crack.

The crack initiation plots of both amorphous and bi-axially oriented PMMA are shown in Fig. 2. One value of initiation time was obtained from each successful experiment, thus each point in the initiation plots represents a single test. Similarly, Fig. 3 represents the crack propagation plots for both materials. At least five sets of test data were plotted for each 'in-air' and 'in-environment' curve. A crack growth interval of 0.1 mm was recorded and plotted in the crack propagation plots. In addition, Table 3 presents the values of the intersection points in each plot. The intersections of the 'in-air' and 'in-environment' curves indicate the value of critical initiation time, t_i^*, critical crack speed, $\dot{a}^*$ and their corresponding fracture energies, G_c from the initiation and propagation plots respectively.

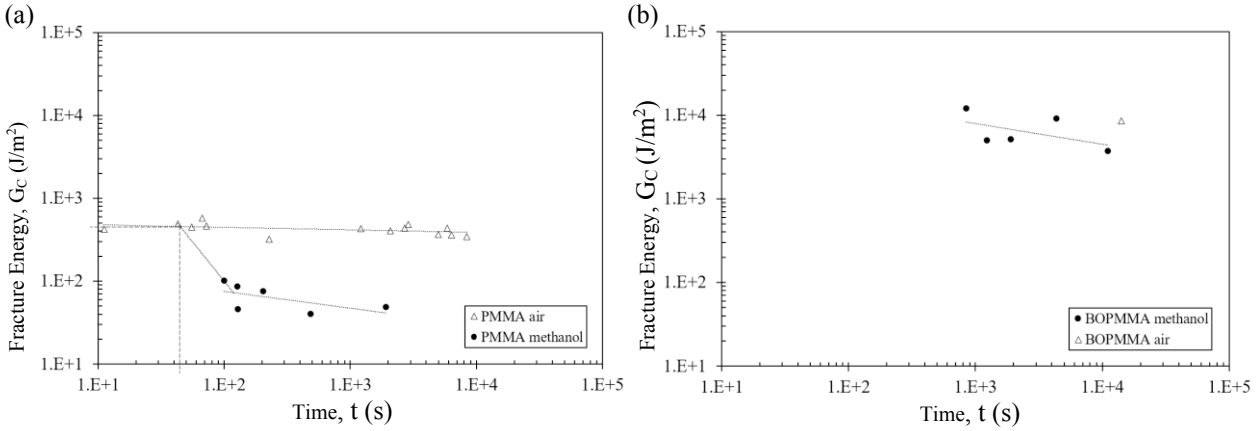

Fig. 2. Initiation G vs time plot for (a) amorphous PMMA and (b) BOPMMA.

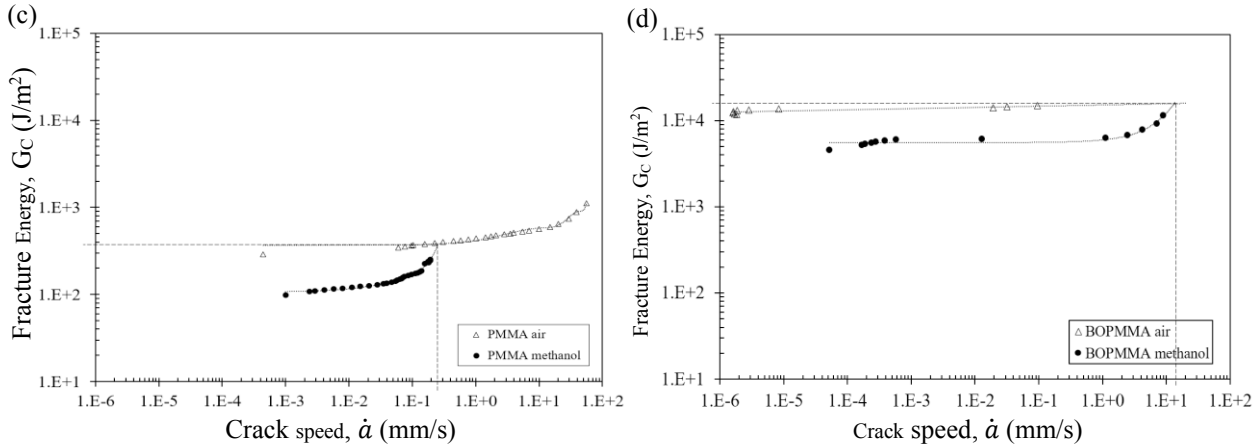

Fig. 3. Propagation G vs crack speed for (a) amorphous PMMA and (b) BOPMMA.

Table 3. Initiation time and crack speed with its corresponding G values.

Materials	Critical initiation time, t_i^* (s)	Critical crack initiation energy G_i^* (J/m^2)	Critical crack speed, $\dot{a}^*$ (mm/s)	Critical crack propagation energy G_p^* (J/m^2)
PMMA	1.34×10^2	1.42×10^1	1.13×10^{-1}	1.28×10^2
BOPMMA	N/A	N/A	1.03×10^1	1.04×10^4

As suggested from the amorphous PMMA results, the initial load and thus the initial fracture energy applied to the specimens in methanol are significantly lowered than those performed in air. However, there is not enough evidence to suggest that methanol has the same effect on BOPMMA. Once the crack has initiated, the energy required to propagate the crack in methanol is lower than in air until it becomes flow controlled. Above this critical point, the availability of the environment becomes the limiting factor, so the crack growth in the environment is equivalent to 'in-air'. This happens at the intersection point of the air and methanol curve in the propagation plots. The factor β, defined by (Chan 1982), as the ratio between $G_{methanol}$ and G_{air} , is found to be 0.25 and 0.40 for PMMA and BOPMMA respectively. The results show that BOPMMA has greater resistance to ESC than amorphous PMMA. This is probably due to the aligned polymer chains of BOPMMA having less free volume and hence a lower flow velocity within the polymer. Both critical crack speed, $\dot{a}^*$ and critical crack propagation energy, G_p^* have increased two orders of magnitude from its amorphous to biaxially orientated structure.

3.4. Fractography

The SEM images in Fig. 4 were taken in vicinity of the relaxation controlled region (region I) with downwards crack growth to examine the fracture mechanism of ESC. In the case of the amorphous PMMA, the presence of methanol has resulted a rougher fracture surface compared to the 'in-air' specimen.

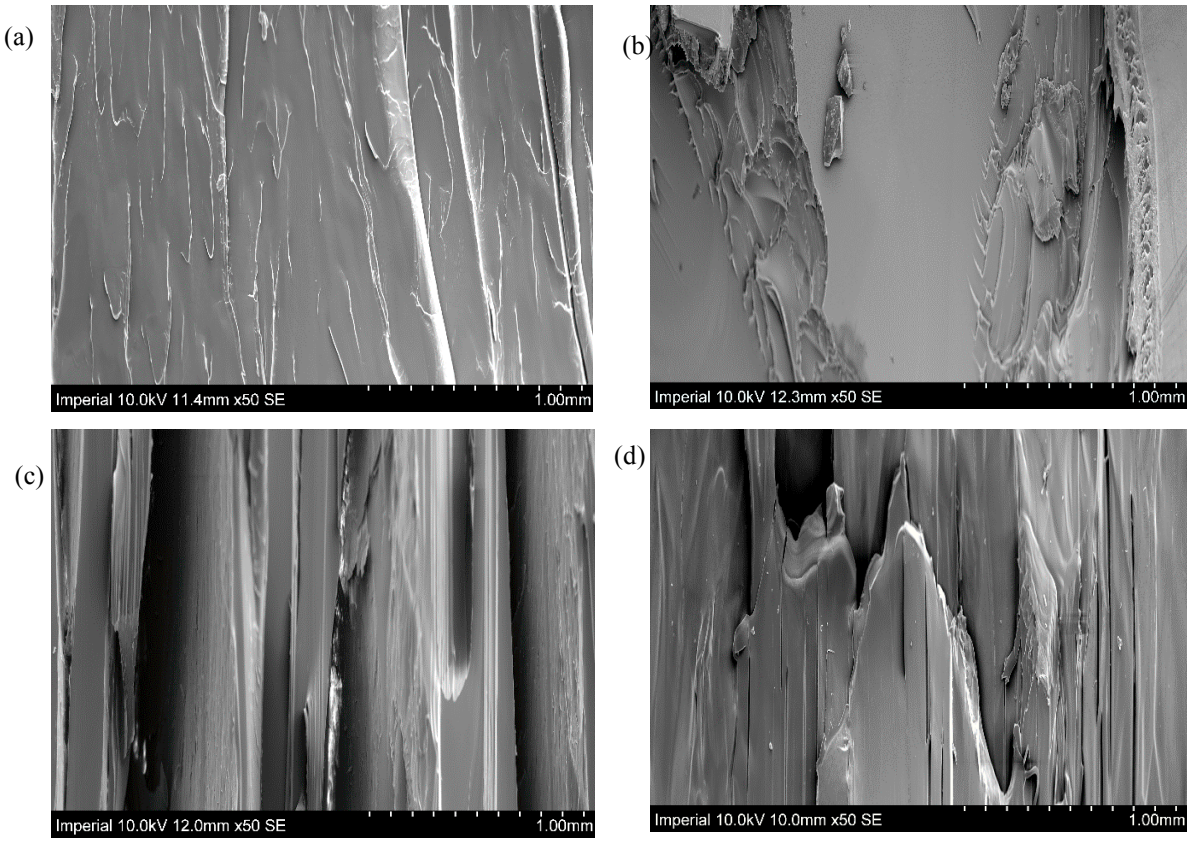

Fig. 4: SEM image of the relaxation controlled region (region I) of (a) PMMA in air, (b) PMMA in methanol, (c) BOPMMA in air and (d) BOPMMA in methanol. The direction of crack growth is downwards.

This again suggests that the effect of crazing is more dominant in methanol. Moreover, both SEM images from the BOPMMA fracture surfaces have shown high alignment along the direction of crack growth and appeared to be significantly rougher in comparison to those found on the amorphous PMMA. The former may suggest a high degree of polymer chain alignment from the biaxial stretching process; the latter agrees closely and is reflected by the increase in fracture energy required for crack initiation and propagation from amorphous PMMA to BOPMMA during ESC as more energy is required to generate larger (i.e. rougher) fracture surfaces.

4. Conclusions

The biaxial stretching process used on PMMA has greatly increase the polymer chain alignment from its amorphous state. This is suggested from the scanning electron microscopy (SEM) images taken from the fracture surfaces of the biaxially oriented PMMA showing high alignment along the direction of crack propagation compared to the amorphous PMMA. With less free volume available in BOPMMA, the polymer has a lower flow velocity within its structure and hence a greater resistance to crazing in methanol. The improved ESC resistance on BOPMMA and thus an increase in fracture energy were also reflected by the rougher fracture surfaces associated with the biaxial effect. Furthermore, the resultant microstructure of the biaxially oriented polymer benefits an improvement of the overall material fracture properties in the directions of stretch. At a mean orientation degree of 70%, the tensile strength of the BOPMMA increased to 91.90 MPa from 81.48 MPa; the fracture toughness, K_C and energy, G_C have increased from 1.01 MPa$\sqrt{m}$ to 2.50 MPa$\sqrt{m}$ and 484 J/m^2 to 1710 J/m^2 respectively. Lastly, the environmental stress cracking (ESC) results have also shown good promise of increase in ESC resistance with the biaxial orientation. The critical crack speed has increased to 1.03x10^1 mm/s at 70% of mean orientation degree from 1.13x10^{-1} mm/s and the critical crack propagation energy to 1.04x10^4 J/m^2 from 1.28x10^2 J/m^2. Similarly, the plasticisation factor, β has increased to 0.40 from 0.25 for the amorphous and biaxially oriented PMMA respectively. All of the above have provide strong evidence to conclude that BOPMMA has a greater resistance to ESC for the ‘in-air’ and ‘in-methanol’ environment, hence a longer component life expectance than the amorphous PMMA.

Acknowledgements

We wish to thank BIAM (Beijing International Aeronautical Materials Corp.) for financial support.

References

Alexander, James, and Charles Atteck. 2009. “Development of Techniques for Lifetime Prediction of Polyethylene Resins for the Water and Gas Industry”. PhD Thesis, Department of Mechanical Engineering, Imperial College London.

Axilrod, B M, M A Sherman, V Cohen, and I Wolock. 1952. “Effects of Moderate Biaxial Stretch-Forming on Tensile and Crazing Properties of Acrylic Plastic Glazing 1.” *Journal Of Research Of The National Bureau Of Standards* 49 (5): 331–43.

Chan, M. K V. 1982. “Fracture Toughness Testing and Slow Crack Growth in Polyethylenes”. PhD Thesis, Department of Mechanical Engineering, Imperial College London.

Chan, M. K V, and J. G. Williams. 1983. “Slow Stable Crack Growth in High Density Polyethylenes.” *Polymer* 24 (2): 234–44.

ISO 13586. 2000. “Plastics — Determination of Fracture Toughness (GIC and KIC) — Linear Elastic Fracture Mechanics (LEFM) Approach.” International Standards Organisation, Geneva.

ISO 527-1:2012. 2012. “BSI Standards Publication Plastics — Determination of Tensile Properties Part 1 : General Principles,” International Standards Organisation, Geneva.

Kamaludin, M. A., Y. Patel, J. G. Williams, and B. R.K. Blackman. 2017. “A Fracture Mechanics Approach to Characterising the Environmental Stress Cracking Behaviour of Thermoplastics.” *Theoretical and Applied Fracture Mechanics*. Elsevier Ltd.

M.Rink, R.Frassine, P.Mariani, and G.Carianni. 2003. “Effects of Detergent on Crack Initiation and Propagation in Polyethylenes.” *European Structural Integrity Society* 32: 103–104.

Wang, X. K., S. C. Wei, B. S. Xu, Y. Chen, X. Yan, and H. H. Xia. 2015. “Transparent Organic Materials of Aircraft Cockpit Canopies: Research Status and Development Trends.” *Materials Research Innovations* 19

Williams, J. G. 1984. "Fracture Mechanis of Polymer″. New York, Chichester, E Horwood.

Williams, J. G., and G. P. Marshall. 1975. “Environmental Crack and Craze Growth Phenomena in Polymers.” *Proceedings of the Royal Society of London. A. Mathematical and Physical Sciences* 342 (1628): 55–77.